

# Sequencing-free On-chip detection of lung cancer by fluorescent enzymatic profiling of cfDNA methylation

Received: 31 July 2025

Accepted: 30 May 2026

Cite this article as: Agbarya, A., Gilat, N., Michaeli, Y. *et al.* Sequencing-free On-chip detection of lung cancer by fluorescent enzymatic profiling of cfDNA methylation. *npj Precis. Onc.* (2026). <https://doi.org/10.1038/s41698-026-01547-2>

Abed Agbarya, Noa Gilat, Yael Michaeli, Jasline Deek, Assaf Grunwald, Sivan Yogev, Lynne Itelson, Suheil Artul, Rasha Khoury, Michael Peled & Yuval Ebenstein

We are providing an unedited version of this manuscript to give early access to its findings. Before final publication, the manuscript will undergo further editing. Please note there may be errors present which affect the content, and all legal disclaimers apply.

If this paper is publishing under a Transparent Peer Review model then Peer Review reports will publish with the final article.

## Sequencing-free On-chip detection of lung cancer by fluorescent enzymatic profiling of cfDNA methylation

Abed Agbarya<sup>1,2</sup>, Noa Gilat<sup>3†</sup>, Yael Michaeli<sup>3†</sup>, Jasline Deek<sup>3</sup>, Assaf Grunwald<sup>3</sup>, Sivan Yogev<sup>3</sup>, Lynne Itelson<sup>4</sup>, Suheil Artul<sup>5</sup>, Rasha Khoury<sup>1</sup>, Michael Peled<sup>6,7</sup> and Yuval Ebenstein<sup>3,8\*</sup>

1 Department of Oncology, Bnai Zion Medical Center, Haifa, Israel; 2 Rappaport faculty of medicine, Technion, Haifa, Israel; 3 School of Chemistry, Sackler Faculty of Exact Sciences, Tel Aviv University-Tel Aviv, Israel; 4 JaxBio Technologies LTD, Netanya, Israel; 5 Department of Radiology, EMMS Hospital, Bar Ilan University Faculty of Medicine, Nazareth, Israel; 6 Institute of Pulmonary Medicine, Chaim Sheba Medical Center, Ramat Gan, Israel; 7 Faculty of Medical & Health Sciences, Tel Aviv University, Tel Aviv, Israel; 8 Department of Biomedical Engineering, Tel Aviv University, Israel

† Currently at JaxBio Technologies LTD.

\* To whom correspondence should be addressed. Email: [uv@tauex.tau.ac.il](mailto:uv@tauex.tau.ac.il).

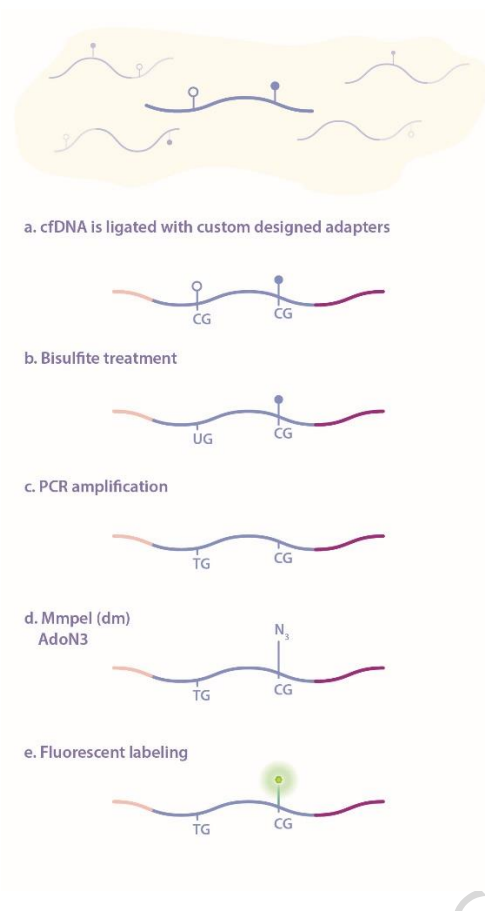
### Abstract:

We present a highly sensitive, low-cost approach for detecting lung cancer and monitoring response to therapy, based on sequencing-free detection of methylation biomarkers in cell-free DNA. After bisulfite treatment and PCR amplification of cell-free DNA, an engineered methyltransferase is used to fluorescently label all originally methylated CpG sites. Labeled cell-free DNA is then analyzed on a standard hybridization microarray. In a proof-of-concept lung cancer study involving 103 participants, we distinguished patients with cancer from healthy individuals with both sensitivity and specificity exceeding 90 % for stage 2-4 lung cancer.

### Main Text:

Lung cancer remains the foremost cause of cancer-related mortality globally<sup>1</sup>. The use of low-dose CT (LDCT) for early detection has shown considerable promise in lowering death rates, as evidenced by studies like the National Lung Screening Trial (NLST)<sup>2</sup> and the Dutch-Belgian Lung Cancer Screening Trial (NELSON)<sup>3</sup>. However, a major issue with LDCT screening is that numerous, mostly benign, nodules are seen in the lungs during screening, leading to high incidence of false-positive results, which can lead to unnecessary biopsies or surgeries. For example, the NLST reported a 26.3% false-positive rate for initial screenings<sup>4</sup>, while the NELSON trial noted a 19.8% rate. In addition, detected lung nodules smaller than 2 cm pose significant challenges for effective biopsy<sup>5</sup> and are usually monitored without intervention. Consequently, tumours may develop resistance or metastasize during this period<sup>6</sup>.

Beyond LDCT screening, liquid biopsies may detect biomolecular signatures, offering potential insights into disease status. Tumour-informed tests such as the recently approved Signatera™ lung cancer test<sup>7</sup>, already achieve remarkable sensitivity for relapse and residual disease detection. However, they require a biopsy to determine tumour-specific mutations. When the tumour is not available, cell-free DNA methylation is emerging as a promising biomarker, exhibiting unique signatures at multiple genomic regions in lung cancer patients compared to healthy individuals, and demonstrating significant diagnostic



value<sup>8</sup>. Nonetheless, many current liquid biopsies lack the sensitivity required for reliable identification of early-stage or low tumour burden cancers. A more tangible entry point for liquid biopsy is in combination with imaging as a molecular complement. The combined evaluation of CT and cfDNA methylation features in lung cancer cases has not been extensively studied. However, recent successful applications of such multimodal data have been used to assess the staging and risk prediction capabilities of cfDNA methylation sequencing combined with imaging<sup>9, 10</sup>. The need for a facile and complementary molecular test is emphasized by the low adherence to LDCT screening, which is currently on the order of ~60%<sup>11,12</sup>.

Current and emerging DNA methylation-based tests rely on DNA sequencing<sup>13,14</sup>. However, the sample enrichment and preparation procedures, the depth of sequencing needed for accurate classification, and the cumbersome computational analysis render these tests inherently expensive. Given these facts, the cost-benefit of such tests for screening or assisting LDCT is unclear<sup>15</sup>. Here we present a novel, sequencing-free microarray method that generates a differential methylation signal pattern, enabling highly accurate, low-cost and specific classification of lung cancer from plasma-derived cell-free DNA

### Discovery of differential methylation signatures in lung cancer samples

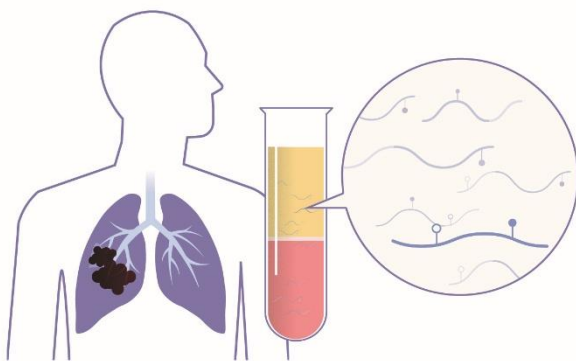
The study was designed to first establish a detectable and classifiable signal between advanced NSCLC and healthy individuals, providing the necessary foundation before assessing performance in more complex, heterogeneous clinical populations. Given that over 40% of Non-Small Cell Lung Cancer (NSCLC) cases are diagnosed at stage four<sup>16</sup>, even a mild shift in staging at diagnosis is expected to benefit patients and physicians. We enrolled 103 participants (Table S1) with available preoperative blood plasma samples for cfDNA extraction and analysis. Among them, 51 patients were diagnosed with stage 2-4 lung cancer, and 52 were age-matched controls.

DNA methylation profiling of these samples was enabled by our recently reported DNA methylation detection chemistry, a chemoenzymatic reaction that introduces a fluorescent reporter to every unmodified methylation site (CpG) in DNA<sup>17-19</sup>. We hypothesized that this may serve to label all positions of methylated CpG sites in bisulfite-treated, PCR-amplified cell-free DNA. Since only methylated CpG sites in the original sample become unmethylated CpGs in the amplified sample, only the originally methylated sites are fluorescently labeled by the enzyme (Figure 1.).

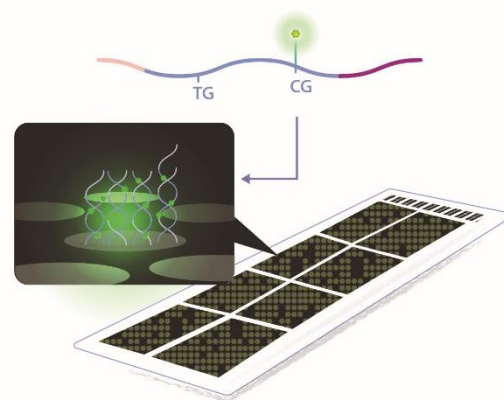
When applying such labeled DNA to a conventional microarray, the fluorescence intensity from each scanned feature reports on the degree of methylation in a specific genomic target defined by the sequence of the capture probes on the array. As proof of concept, we used a commercially available comparative genomic hybridization array (CGH) from Agilent Technologies, designed for copy number

analysis. As such, it sparsely covers the entire genome at ~40kb intervals and is denser in gene bodies and regulatory elements, with a total of about 60k genetic loci represented on the array surface. Fluorescently labeled cfDNA samples were prepared for hybridization (see methods), applied to the arrays, and scanned after overnight hybridization. Following data normalization, an analytical pipeline was built to identify distinctive methylation loci. For training, we used data acquired from 22 lung cancer samples and 21 healthy controls. A model was built to analyze the methylation patterns and optimized through leave-one-out cross-validation to identify a set of 170 genomic regions with highly differential methylation levels that allowed us to distinguish the two populations with high accuracy. The experimental and analytical workflow is illustrated in Figure 2.

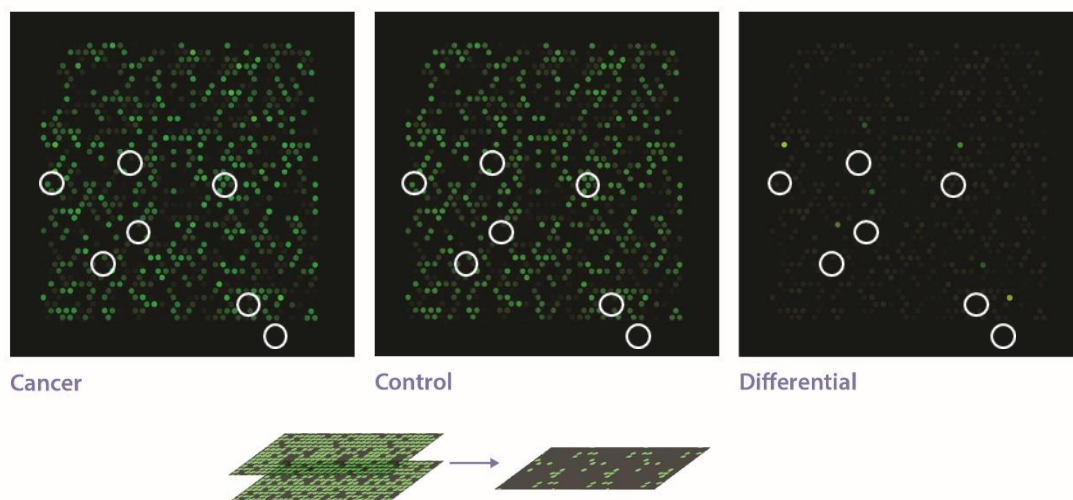
#### a. Blood draw



#### b. DNA extraction and labeling



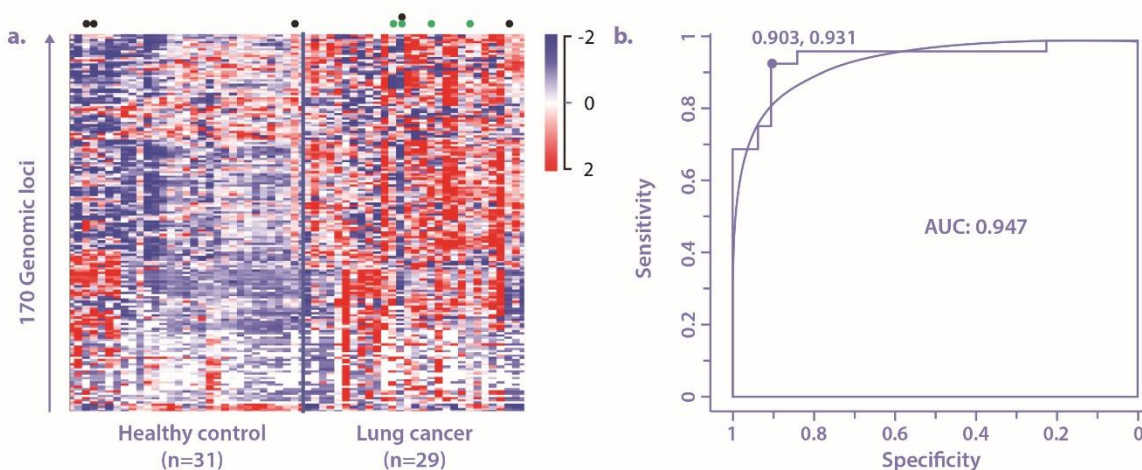
#### c.



#### Blind validation and classification performance

Next, a test set composed of 29 lung cancer samples and 31 controls was blindly classified using the selected biomarker panel. The heatmap in Figure 3a displays the top 170 differential regions across 60 samples tested, showing high contrast between the two populations (see SI for more details on the scoring

system). Receiver operating characteristic (ROC) analysis showed peak performance of 93.1% sensitivity at 90.3% specificity, with an area under the curve (AUC) of 0.947 (Figure 3b). It is critical to note that the reported specificity was achieved against a healthy control group and does not represent the expected performance in a clinical setting where distinguishing cancer from benign lung disease is paramount. This value is likely an overestimation of the test's real-world specificity but provides solid grounds for further development.



### Lung cancer subtype classification and biological relevance

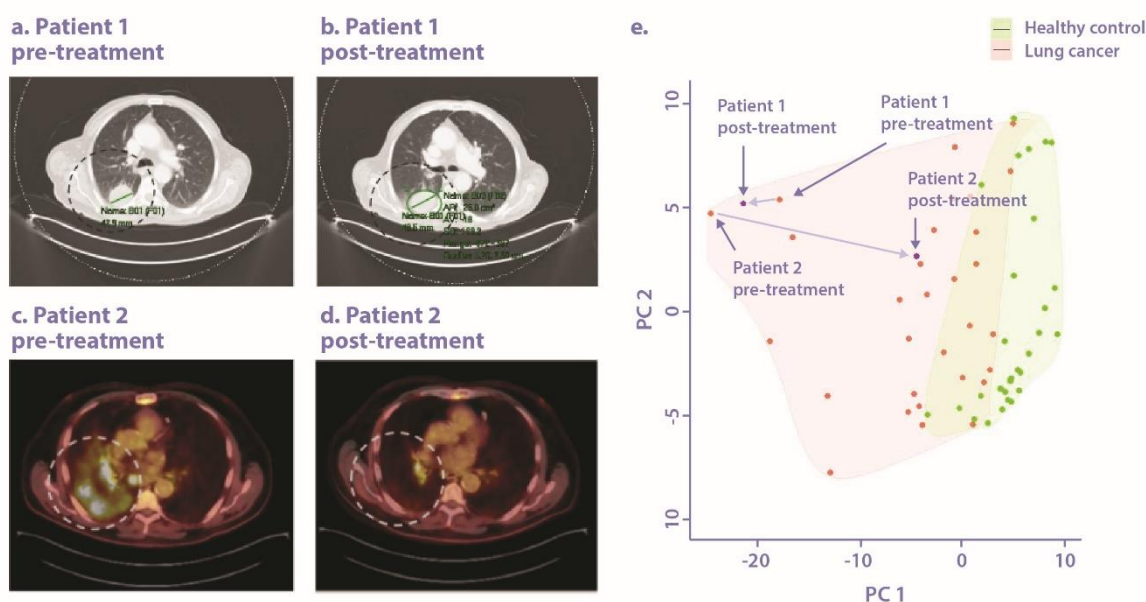
To further test the potential of this new assay for cancer subtyping we investigated unique methylation patterns within the patient group. Our NSCLC cohort was composed of two histologic subtypes, adenocarcinoma (N=32) and squamous cell carcinoma (N=17). Independent comparison of the squamous cell signatures to 22 age matched adenocarcinoma patient signatures, revealed a set of 168 methylation markers (not included in the cancer/healthy classifier) that distinguishes between these histological subtypes with an AUC of 0.881, correctly classifying 86.4% of squamous cell carcinoma samples, and 88.2% of adenocarcinoma samples (Figure S1).

For mechanistic validations that our selected differential panel is biologically associated with lung cancer we analyzed the panel for involved genes and biological pathways. Since many of our biomarkers reside outside gene coding regions, we used GREAT<sup>20</sup> to generate a list of associated genes through proximity or functional interpretation of *cis*-regulatory elements. Among the genes identified were several established oncogenic drivers and tumor suppressors in lung cancer such as BRAF<sup>21</sup>, CDKN2B<sup>22</sup>, SMARK<sup>23</sup> and RICTOR<sup>24</sup>, as well as several EMT/metastasis regulators such as SNAI1<sup>25</sup>, Vimentin<sup>26</sup>, ROCK<sup>27</sup>, TRIB2<sup>28</sup> and FYN<sup>29</sup>. We then used DAVID<sup>30</sup> for signaling pathway enrichment. Stringent analysis yielded two highly significant pathways, Developmental protein (UniPort: KW-9996 & KW-0217) and cyclic adenosine monophosphate (cAMP) signaling (UniPort: hsa04024). Both pathways are directly involved in many cancers and specifically in lung cancer. The developmental module, that contains WNT /  $\beta$ -catenin signaling, includes dozens of genes from our biomarker list, including TCF7L2 (alias TCF-4) which is known to modulate WNT signaling in lung cancer<sup>31</sup>. Other markers were related to the cAMP signaling pathway in lung cancer, most notably GNAS, whose hotspot R201C/H mutations characterize a distinct subset of mucinous and

non-mucinous lung adenocarcinomas, and VIPR1 (alias VPAC1) which is over-expressed in 58 % of NSCLC and SCLC tumours<sup>32</sup> (see supplementary information and supplemental file 1).

### Monitoring response to therapy

Initial evidence suggests the potential of the assay to monitor treatment response in NSCLC patients as a molecular complement to radiology. We followed two cases of advanced stage NSCLC requiring an aggressive chemo-immunotherapy (9LA) protocol. Extracted cfDNA methylation was analyzed before and after treatment, alongside chest imaging. Good correlation was observed between the clinical response evaluated by CT or PET-CT and the methylation levels in the differential loci (Figure 4). Patient 1 did not respond to the treatment and showed a slight increase in tumor burden (Figure 4. a-b). When placed on a PCA plot based on the patient methylation array data, slight regression is observed. This patient did not exhibit significant change in their methylation profile (Figure 4.e). Patient 2, on the other hand, responded well to the treatment. The PET-CT scan shows pathological uptakes in multiple malignant masses of NSCLC in the right lung, that are almost diminished after 4 cycles of treatment (Figure 4. c-d, white circle). When placed on the PCA plot, a distinct shift in the methylation signature toward the healthy control cluster is observed (Figure 4.e). While these results are promising, the small sample size (n=2) limits generalizability. Further validation in a larger cohort is necessary to establish the reliability of this method for monitoring treatment response.



This study demonstrates the potential of our methylation microarray approach in advanced-stage lung cancer. Our use of a separate validation set and blinded analysis provides a strong foundation for the potential of this method, setting the stage for future large-scale validation studies. While promising, these results lay the groundwork for crucial future validation in early-stage patients, which will be essential for realizing the full clinical potential of this method for early detection and for complementing chest imaging with molecular information. The test may be performed at the point of care in a simple and cost-effective manner and yielded biologically relevant targets. We note that we have only examined a small fraction of

the DNA methylation landscape, limited by the CGH arrays used. Nevertheless, it presents a readily available low-cost alternative to other methylation arrays and methylation sequencing. Currently, the test is performed within 2-3 days and costs ~60 USD/sample when performed on commercially available 24-sample arrays from Agilent Inc. A significant advantage of the proposed approach over existing methylation arrays is its ability to sample a methylation region rather than a specific CpG, resulting in integrated fluorescent intensity from a target region that displays much higher signal to noise ratio (SNR). The methylation atlas has established that CpG methylation occurs in blocks and that these block patterns are cell-type specific<sup>33</sup>. This fact comes to our advantage as it aligns perfectly with the experimental readout of the method. We are currently performing such biomarker discovery on a larger scale, followed by printing a dedicated lung cancer array that will be accessible to the research and clinical community. A larger prospective clinical trial (LUMEN; Eu 101188111) is currently finalizing a protocol for evaluating the test in predicting tumor response to systemic treatment.

## **Methods:**

### **Ethical approval**

The study was conducted in accordance with the Declaration of Helsinki and good clinical practice guidelines following approval by ethics committees and institutional review boards at EMMS (EMMS Hospital Nazareth; Approval number: 37-22-EMMS). All participants provided written informed consent.

### **Sample collection and processing**

Whole blood samples (4-8 mL) were collected in Streck tubes (STRECK) to ensure cfDNA stabilization. Plasma was separated by centrifugation in two steps: first at 1600g for 10 minutes, followed by careful transfer of the upper plasma layer to a new 15 mL tube without disturbing the buffy coat. A second centrifugation was performed at 5000g for 10 minutes to further purify the plasma. cfDNA was extracted using Apostle MiniMax High Efficiency Cell-Free DNA Isolation Kit according to the manufacturer's instructions. Following extraction, cfDNA underwent adapter ligation using the NEBNext Ultra II End Prep kit (New England Biolabs) with custom adapters to prepare for downstream processing. Bisulfite conversion was performed with the EZ-DNA methylation Gold kit (Zymo Research) to enable differentiation between methylated and unmethylated cytosines. The converted cfDNA was amplified via PCR under the following conditions: 95°C for 2 minutes, followed by 18 cycles of 95°C for 15 seconds, 55°C for 15 seconds, and 72°C for 30 seconds. A final extension was performed at 72°C for 2 minutes, and samples were held at 12°C indefinitely. PCR products were cleaned using AMPure beads (bead ratio 1.2x, 60 µL), and DNA was eluted in 30µl for downstream labeling and hybridization.

### **Fluorescent labeling**

The “magic sauce” enabling this assay is the use of a bacterial CpG methyltransferase (M.MpeI) that was mutated to allow the transfer of an azide residue to every CpG in the amplified sample<sup>19</sup>. A fluorophore is clicked on to the azide resulting in light emission from every site that was methylated in the original cfDNA (unmethylated CpGs will turn to TpGs and will not be labeled).

Bisulfite-converted and amplified cfDNA samples underwent fluorescent labeling process according to Avraham et al<sup>19</sup>. Analysis of efficiency of labeling and its correlation with methylation level is presented in Figures S3-S5.

### **DNA Microarray Hybridization and scanning**

When applying the sample to a microarray, each array locus emits light in proportion to the amount of methylated CpGs in the original cfDNA sample, generating a unique light intensity pattern that represents the underlying sample methylome. The assay is inherently targeted via hybrid capture on the microarray surface, resulting in an extremely simple and low-cost test to perform and analyze. After bisulfite conversion, most genomic cytosines are converted and thus may hamper specific hybridization to the array. However, the low G content in the array probes (<15%) ensure specificity despite the conversion process (Figure S2).

Following fluorescent labeling, 500 ng of the labeled cfDNA amplicons were hybridized onto Agilent 60K Human CGH microarrays (Agilent Technologies). Pre-hybridization solution was prepared in a 50 mL tube by combining 0.5 g BSA (Sigma), 41 mL double-distilled water (DDW), 8.75 mL SSC 20x, and 250  $\mu$ L SDS 20%. Agilent microarray slides were incubated in the pre-hybridization solution at 37°C for 20 minutes. Labeled cfDNA samples were prepared with 2X Agilent hybridization buffer. A total volume of 100  $\mu$ L was prepared by mixing 50  $\mu$ L of labeled DNA with 50  $\mu$ L of Agilent 2X hybridization buffer. Samples were incubated at 98°C for 3 minutes and then incubated at 37°C for 30 minutes before hybridization onto the Agilent array. Buffer composition and hybridization temperature were optimized for specific and consistent signal generation. It was performed overnight at 48°C with mild rotation to ensure efficient and uniform binding of cfDNA to complementary probes on the array surface. Post-hybridization, the microarrays were washed twice with PBST for 1 minute to remove non-specifically bound DNA. The slides were scanned using the Innoscan 1100 scanner (Innopsys), and fluorescence signal intensities were background subtracted and quantified with the Mapix software (Innopsys).

### **Data analysis**

A custom analytical pipeline was developed to enable the simultaneous processing of a large number of datasets. The pipeline consists of two main modules: preprocessing and training with feature selection. This pipeline is utilized in both the training and testing.

#### **(i) Preprocessor Module:**

To address potential biases arising from data heterogeneity, array-specific variations, or differences in sample conditions, robust preprocessing procedures are applied consistently during both the training and testing stages. The initial step in preprocessing involves normalizing the array fluorescence intensity data.

The normalization strategy leverages the observation that over 99% of methylation sites on the CGH arrays are consistent across all arrays and samples, and it relies on the internal calibration probes embedded within the arrays. After evaluating several approaches, polynomial fitting was identified as the most effective normalization method, successfully producing uniform illumination levels across all slides. This process achieved over 99% similarity between any two compared samples. To minimize batch effects, each slide was loaded with an equal number of cancer and healthy samples. Furthermore, multiple experiments were conducted across different slides and at different times to differentiate true biological

signals from technical variability. To ensure robustness, both the training set and the test set were composed of a diverse selection of samples originating from all slides.

(ii) Training and Feature Selection Module:

To identify differential methylation markers distinguishing healthy from lung cancer samples, a statistical T-test was performed with a significance threshold of  $p < 0.01$ . In addition, only features showing a differential methylation ratio greater than 20% between the two groups were selected, resulting in a final set of 150–200 features capable of discriminating between healthy and lung cancer samples. A training cohort comprising 21 healthy and 22 lung cancer cfDNA samples was used for marker discovery and model training. A simple classification process was followed. The methylation level of every biomarker in the tested sample is compared to the average methylation level of the same feature in the training cohorts. A value of 1 is given to this feature if it is closer to the healthy methylation level and a weight of 0 if it is closer to the lung cancer methylation value. Next, for each sample, a score is calculated by summing all the assigned values (of all selected methylation features), with each feature contributing equally; samples are classified as lung cancer or healthy based on whether their score falls above or below a predefined threshold.

Subsequently, an independent validation set of 29 lung cancer and 31 healthy cfDNA samples, not included in the training phase, was analyzed to evaluate the model's performance. Based on their methylation profiles, each sample was assigned a score classifying it as either healthy or lung cancer (Figure S7). Specificity and sensitivity were calculated from the blind-testing results, providing a quantitative assessment of the assay's diagnostic accuracy (Table S2). A similar process was applied to identify markers that differentiate between lung adenocarcinoma and squamous cell carcinoma.

### Data availability

All data is contained within the main text and the supplementary file.

### Acknowledgments

This work was supported by the European Research Council consolidator grant [number 817811]; Israel Science Foundation [grant number 771/21]; Nicholas and Elizabeth Slezak Super Center for Biomedical Engineering at Tel Aviv University; Dotan Cancer Biology Research Center, Tel Aviv University; European Innovation Council Accelerator grant [number 101188111].

### Author contribution

A.A., S.A., R.K., and M.P. contributed to patient recruitment, clinical characterization, and provided clinical samples and medical input. N.G., Y.M., and Y.E. conceived and designed the study. N.G., Y.M., L.I., and J.D. performed the experiments. N.G., Y.M., A.G., L.I., and S.Y. carried out data processing, statistical analysis, and computational analyses. Y.E., Y.M., N.G., and J.D. interpreted the results and wrote the manuscript. All authors reviewed, edited, and approved the final version of the manuscript.

### Competing interests

The intellectual property underlying the technology described in this manuscript has been licensed to a newly formed spinout company, JaxBio Technologies LTD. YE is a founder and holds equity in JaxBio

Technologies LTD. AA serves as a scientific consultant to the company. YM and NG are currently employed by the company. The other authors do not have a competing interest.

Pending patents: The technology described in this manuscript is covered by a pending patent application PCT/IL2021/050706, filed by Ramot at Tel Aviv University Ltd. as the applicant. The listed inventors are Yuval Ebenstein, Shahar Zirkin, Yael Michaeli Hoch, Noa Gilat, Orit Feldstein, and Adaya Ben-Moshe. The patent relates to methods and systems for the sequencing-free detection of cancer-associated DNA methylation patterns in cell-free DNA using chemical labeling and microarray-based analysis, which directly underpin the experimental approach, assay design, and analytical framework described in this manuscript. The relevant intellectual property has been exclusively licensed to JaxBio Technologies Ltd.

ARTICLE IN PRESS

## References

1. Siegel, R. L., Miller, K. D., Wagle, N. S. & Jemal, A. Cancer statistics, 2023. *CA. Cancer J. Clin.* **73**, 17–48 (2023).
2. Reduced Lung-Cancer Mortality with Low-Dose Computed Tomographic Screening | New England Journal of Medicine. <https://www.nejm.org/doi/10.1056/NEJMoa1102873>.
3. Koning, H. J. de *et al.* Reduced Lung-Cancer Mortality with Volume CT Screening in a Randomized Trial. *N. Engl. J. Med.* **382**, 503–513 (2020).
4. The National Lung Screening Trial Research Team, Results of Initial Low-Dose Computed Tomographic Screening for Lung Cancer. *N. Engl. J. Med.* **368**, 1980–1991 (2013).
5. Andrade, J. R. de *et al.* CT-guided percutaneous core needle biopsy of pulmonary nodules smaller than 2 cm: technical aspects and factors influencing accuracy. *J. Bras. Pneumol.* **44**, 307–314 (2018).
6. Zhong, D. *et al.* Lung Nodule Management in Low-Dose CT Screening for Lung Cancer: Lessons from the NELSON Trial. *Radiology* <https://doi.org/10.1148/radiol.240535> (2024)  
doi:10.1148/radiol.240535.
7. Lebow, E. S. *et al.* ctDNA-based detection of molecular residual disease in stage I-III non-small cell lung cancer patients treated with definitive radiotherapy. *Front. Oncol.* **13**, (2023).
8. Ezeogbu, M. *et al.* Cell-free DNA methylation in the clinical management of lung cancer. *Trends Mol. Med.* **30**, 499–515 (2024).
9. Yang, M. *et al.* Enhancing the differential diagnosis of small pulmonary nodules: a comprehensive model integrating plasma methylation, protein biomarkers, and LDCT imaging features. *J. Transl. Med.* **22**, 984 (2024).
10. Liang, W. *et al.* A clinically effective model based on cell-free DNA methylation and low-dose CT for risk stratification of pulmonary nodules. *Cell Rep. Med.* **5**, (2024).

11. Lin, Y. *et al.* Patient Adherence to Lung CT Screening Reporting & Data System—Recommended Screening Intervals in the United States: A Systematic Review and Meta-Analysis. *J. Thorac. Oncol. Off. Publ. Int. Assoc. Study Lung Cancer* **17**, 38–55 (2022).
12. Lopez-Olivo, M. A. *et al.* Patient Adherence to Screening for Lung Cancer in the US: A Systematic Review and Meta-analysis. *JAMA Netw. Open* **3**, e2025102 (2020).
13. Klein, E. A. *et al.* Clinical validation of a targeted methylation-based multi-cancer early detection test using an independent validation set. *Ann. Oncol.* **32**, 1167–1177 (2021).
14. Liu, M. C. *et al.* Sensitive and specific multi-cancer detection and localization using methylation signatures in cell-free DNA. *Ann. Oncol.* **31**, 745–759 (2020).
15. Oncology, T. L. Cancer detection: the quest for a single liquid biopsy for all. *Lancet Oncol.* **21**, 733 (2020).
16. American Cancer Society. *Facts & Figures 2025*. <https://www.cancer.org/cancer/types/lung-cancer/about/key-statistics.html>.
17. Sharim, H. *et al.* Long-read single-molecule maps of the functional methylome. *Genome Res.* **29**, 646–656 (2019).
18. Gabrieli, T. *et al.* Chemoenzymatic labeling of DNA methylation patterns for single-molecule epigenetic mapping. *Nucleic Acids Res.* **50**, e92 (2022).
19. Avraham, S. *et al.* Chemo-Enzymatic Fluorescence Labeling Of Genomic DNA For Simultaneous Detection Of Global 5-Methylcytosine And 5-Hydroxymethylcytosine. *ChemBioChem* **24**, e202300400 (2023).
20. Cy, M. *et al.* GREAT improves functional interpretation of cis-regulatory regions. *Nat. Biotechnol.* **28**, (2010).
21. Yan, N. *et al.* BRAF-Mutated Non-Small Cell Lung Cancer: Current Treatment Status and Future Perspective. *Front. Oncol.* **12**, 863043 (2022).

22. HJazi, A. *et al.* CDKN2B-AS1 as a novel therapeutic target in cancer: Mechanism and clinical perspective. *Biochem. Pharmacol.* **213**, 115627 (2023).
23. Papavassiliou, K. A., Anagnostopoulos, N. & Papavassiliou, A. G. Molecular insights into SMARCA2 degradation in SMARCA4-mutant lung cancers. *Trends Cancer* **11**, 185–187 (2025).
24. Cheng, H. *et al.* RICTOR Amplification Defines a Novel Subset of Patients with Lung Cancer Who May Benefit from Treatment with mTORC1/2 Inhibitors. *Cancer Discov.* **5**, 1262–1270 (2015).
25. Li, B. & Li, R. SNAI1: a key modulator of survival in lung squamous cell carcinoma and its association with metastasis. *J. Cardiothorac. Surg.* **19**, 531 (2024).
26. Richardson, A. M. *et al.* Vimentin Is Required for Lung Adenocarcinoma Metastasis via Heterotypic Tumor Cell–Cancer-Associated Fibroblast Interactions during Collective Invasion. *Clin. Cancer Res.* **24**, 420–432 (2018).
27. Barcelo, J., Samain, R. & Sanz-Moreno, V. Preclinical to clinical utility of ROCK inhibitors in cancer. *Trends Cancer* **9**, 250–263 (2023).
28. Grandinetti, K. B. *et al.* Overexpression of TRIB2 in human lung cancers contributes to tumorigenesis through downregulation of C/EBP $\alpha$ . *Oncogene* **30**, 3328–3335 (2011).
29. Peng, S. & Fu, Y. FYN: emerging biological roles and potential therapeutic targets in cancer. *J. Transl. Med.* **21**, 84 (2023).
30. Sherman, B. T. *et al.* DAVID: a web server for functional enrichment analysis and functional annotation of gene lists (2021 update). *Nucleic Acids Res.* **50**, W216–W221 (2022).
31. Nguyen, D. X. *et al.* WNT/TCF Signaling through LEF1 and HOXB9 Mediates Lung Adenocarcinoma Metastasis. *Cell* **138**, 51–62 (2009).
32. Reubi, J. C. *et al.* Vasoactive Intestinal Peptide/Pituitary Adenylate Cyclase-activating Peptide Receptor Subtypes in Human Tumors and Their Tissues of Origin<sup>1</sup>. *Cancer Res.* **60**, 3105–3112 (2000).

33. Loyfer, N. *et al.* A DNA methylation atlas of normal human cell types. *Nature* **613**, 355–364 (2023).

Figure legends:

**Figure 1.** Sample preparation workflow: *a.* Cell-free DNA is ligated with custom adapters. *b.* Bisulfite conversion retains only methylated CpGs. *c.* PCR amplification. *d.* CpGs are enzymatically labeled with an azide. *e.* A fluorophore is clicked onto the CpG. cfDNA cell-free DNA, PCR polymerase chain reaction, dm double mutant, AdoN3 AdoYn-Azide.

**Figure 2.** Experimental process and resulting data. *a.* whole blood is collected and plasma is separated. *b.* Cell-free DNA is extracted from plasma, processed, and fluorescently labeled at methylation sites. Labeled DNA is applied to a hybridization microarray, directly reporting on the methylation status of every genomic region represented on the microarray. *c.* Detecting differential targets: Raw normalized image scans of the same ~1200 feature region in two microarrays: Lung cancer (left) and healthy control (middle). Each feature on the array targets cfDNA from a specific genomic locus. Signal intensity is proportional to the degree of methylation in this locus. A differential image (right) shows only features that display significant detectable differences between the methylation levels in lung cancer versus a healthy control. This small subset of targets is later used to classify lung cancer samples versus controls.

**Figure 3.** Blind validation of cfDNA methylation signatures distinguishing patients with lung cancer from controls. *a.* A heatmap showing the methylation levels of the top 170 differential regions in lung cancer and healthy controls (Z-Score scale). Green dots on the top of the heatmap indicate early-stage cancer and black dots indicate misclassified individuals. *b.* Receiver operating characteristic (ROC) curve reflecting the classification performance on 60 blinded participants. AUC area under the curve.

**Figure 4.** cfDNA methylation profiles reflect response to treatment in lung cancer patients. *a.* The CT scan shows a 42 mm malignant mass (NSCLC) in the Right lung (green section line). *b.* Tumor Progression to 49 mm after 3 cycles of treatment (Non-Response). *c.* PET-CT scan shows multiple masses in the right lung (NSCLC) before starting treatment with chemo-immunotherapy. *d.* Tumor Regression after 4 cycles of treatment (Response). *e.* PCA plot presenting the distribution of lung cancer (red) and healthy controls (green) samples based on the selected methylation biomarkers. The distance between points reflects their overall similarity and the shaded areas are an approximation of the area occupied by each class (cancer in pink and controls in green). Pre- and post-treatment samples are labeled with arrows. Light blue arrows indicate the direction of response to therapy. PC principle component.

ARTICLE IN PRESS